Force of crystallization during the growth of siliceous concretions

Thomas Dewers
Department of Geology, Indiana University
Bloomington, Indiana 47405
Peter Ortoleva
Departments of Chemistry and Geology, Indiana University
Bloomington, Indiana 47405

ABSTRACT

The force of crystallization is of renewed interest as a diagenetic replacement mechanism. We present a quantitative reaction-transport model for mineral replacement driven by the pressure exerted by crystal growth, based on continuum equations accounting for conservation of mass and momentum. A condition of volume-for-volume replacement during growth and dissolution is shown to arise naturally from the interaction of mechanical and reactive deformation. When applied to the postnucleation growth of quartz in a calcite plus amorphous silica host, a centimetre-scale concretion-like feature is shown from our simulations to arise within roughly 17 ka.

INTRODUCTION

A "force of crystallization" is thought to be responsible for phenomena occurring at conditions ranging from surface temperatures and pressures to those characteristic of metamorphic depths. Maliva and Siever (1987, 1988) have cited the force of crystallization as a means for constant volume replacement of calcite by quartz. Buczynski and Chafetz (1987) showed that growth of calcite grains can produce fracturing of quartz grains. Herein we follow up on our previous work (Dewers and Ortoleva, 1989a, 1989b), in which we introduced a reaction-transport model describing the dynamics of the processes of pressure solution and pressure of crystallization. Our aim is to make further connections between the theory and field observations with emphasis on the growth of siliceous concretions from a radiolarian- or sponge-spicule–bearing limestone.

INTERPLAY BETWEEN MECHANICAL AND REACTIVE DEFORMATION

The details of the mechanism of pressure of crystallization have not been clearly defined. Weyl (1959) presented a phenomenological model based on a linear dependence of solubility on stress. Rates of grain growth are in his model proportional to diffusional rates within a thin fluid film. Mineral growth against normal stress was shown to occur given a sufficient degree of supersaturation in the surrounding pore fluid. Other workers have also related the magnitude of pressure during mineral growth to levels of supersaturation in pore fluid but, to date, have been restricted to equilibrium thermodynamics (Maliva and Siever, 1988; Ostapenko and Yaroshenko, 1975). A result of this type, which follows from the pressure dependence of Gibbs free energy (neglecting strain energy), is (Maliva and Siever, 1988)

$$\Omega = \exp \left\{ \frac{\Delta V(P - p)}{RT} \right\} , \tag{1}$$

where Ω is the level of supersaturation of pore fluid above that in equilibrium with the solid at hydrostatic fluid pressure p, ΔV is the difference between the molar volume of solid and solutes, P is normal (nonhydrostatic) stress applied across grain boundaries, R is the gas constant, and T is temperature. This relation gives the P at equilibrium that would result from a departure of Ω from unity. For Ω values >1, $P > p$. Use of equation 1 is restricted in that it is valid only under conditions of equilibrium; as such, P found from this equation must represent some limiting value of normal stress.

Our model consists of coupled partial differential equations of grain growth and dissolution, solute transport, and rock deformation flow due to both dissolution and precipitation and linear viscous creep. We have shown (Dewers and Ortoleva, 1989a) that the interplay between the rates of mineral and fluid reactions, bulk-rock viscosity, and total (macroscopic) effective stress in a low-porosity rock controls the domain of influence of a force-of-crystallization–mediated constant-volume replacement mechanism. This is shown from a Navier-Stokes equation accounting for the distribution of pressure, which, in the case of no imposed rate of strain, isotropic reaction, and Newtonian flow becomes (Dewers and Ortoleva, 1989a)

$$2\vec{\nabla} P^{m} = \eta \nabla^{2} \vec{u} + \frac{1}{3} \eta \vec{\nabla}(\vec{\nabla} \cdot \vec{u}), \tag{2}$$

where

$$\vec{\nabla} \cdot \vec{u} = \sum_{i=1}^{M} n_{i} G_{i}^{v}. \tag{3}$$

Equation 2 is derived by combining a linear viscous constitutive law for stress and strain rate, a force balance condition, and the relation between strain rate and rock deformation velocity; n_i is the number of grains of mineral i per unit volume, $\vec{u}$ is the rock flow velocity, η is the bulk-rock viscosity (assumed constant), P^{m} is the pressure applied to and within a supra–grain-size rock volume element, G_{i}^{v} is the rate of grain volume change due to reaction, and M is the total number of minerals in the system. The usual incompressibility condition of viscous rock flow (i.e., the divergence of the velocity is zero) has been replaced by equation 3 because rock may locally "compress" or "dilate" due to dissolution and growth of mineral grains.

The relative order of magnitude of the terms in equation 2 determines which of two limiting types of behavior best characterizes the system dynamics. For example, if the rock is not very viscous, the right-hand side of equation 2 is negligible compared to the left-hand side, implying constancy in pressure—the Reuss (1929) limit—on the time scale of reaction. Here, crystal growth would result in displacement of its surroundings. If the bulk viscosity is larger than a critical magnitude, the "stiffness" of the rock (relative to the time scale for reaction) implies a volume constraint condition wherein growth of one mineral is restrained to regions of dissolution of another. It is this limit in which we are interested.

Rates of grain/fluid reactions can be written

$$G_i^v \sim -k_i S_i (1 - \Omega_i), \qquad (4)$$

where k_i is the rate coefficient of the forward (dissolution) reaction and S_i is the surface area of i grains, or the area of active dissolution or growth sites on the grain/solution interface. The form of k_i and Ω_i for water-film diffusion-limited reaction rates is givn in Appendix 1. In the case of relatively small pressures, fast reaction rates, and/or high bulk-rock viscosities, the terms on the right-hand side of equation 2 will dominate. Specifically, this can be expressed in terms of a parameter, ξ, where

$$\xi \equiv 3\,\bar{\eta}\bar{n}\bar{S}\bar{k}\,\{1 - \bar{\Omega}\}/2\bar{P}^m. \qquad (5)$$

Here typical or average values are indicated with bars, $\bar{P}^m$ being a typical lithostatic pressure. If $\xi \gg 1$, the latter term in equation 2 will dominate, and thus the distribution of mean stress is controlled by grain growth and dissolution. We showed (Dewers and Ortoleva, 1989a) that in the limit of $\xi \to \infty$ for a closed system,

$$\sum_{i=1}^{M} n_i G_i^v = 0, \qquad (6)$$

which, in the case of a calcite-quartz rock, becomes

$$n_q k_q S_q \{1 - \Omega_q\} = -n_c k_c S_c \{1 - \Omega_c\}. \qquad (7)$$

Thus, quartz growth must in this limit be accompanied by calcite dissolution. The crossover condition $\xi = 1$ gives a relation that may describe the transition between volume-for-volume replacement and "Reuss" behavior. For rocks closer to equilibrium, we find that the force of crystallization becomes less influential with greater depth. In situations where $\xi \ll 1$, crystal growth would proceed by pushing away (not dissolving) the surrounding matrix of grains. This would be the case for a concretion growing in relatively unconsolidated sediment. Both constant-volume replacement and matrix displacement are features associated with concretions and other sedimentary segregations (Pettijohn, 1975); the crossover criteria (equation 5) shows that the occurrence of either behavior will depend on rheological and geochemical parameters.

Equation 7 shows an important relation following from pressure of crystallization effects—that of constant volume replacement. It implies, e.g., if quartz is favored to grow ($\Omega_q > 1$), then calcite must dissolve because the pressure would adjust to a value dictated by reaction rates of both quartz growth and calcite dissolution. In this way, equation 7 serves to fix the pressure of crystallization. As rock flow due to grain-fluid reactions is negligible in large η systems, n_q and n_c are constant if nucleation of new grains is ignored. If we assume they are equal, and assume further for simplicity that the S values are constant and equal, we arrive at the relation

$$\Omega_c = (1 + \frac{k_q}{k_c}) - \frac{k_q}{k_c}\,\Omega_q. \qquad (8)$$

This implies that given a saturation level for calcite, Ω_c, the system will adjust by changing the saturation level of quartz, Ω_q, so that equation 8 is satisfied. Figure 1 is a schematic plot of Ω_q vs. Ω_c as in equation 8. This is a generalization of the result given in equation 1; it accounts for the important role of kinetics (i.e., nonequilibrium) effects inherent to changes induced by pressure of crystallization. The heavy line in Figure 1 is the line satisfied by the volume constraint condition (equation 8). The dashed lines represent hypothetical saturation lines for quartz and calcite. For a given calcite supersaturation Ω_c' in Figure 1, the level of undersaturation resulting between pore fluid and quartz may be determined by following the vertical line from the point designated Ω_c' up to the volume constraint line,
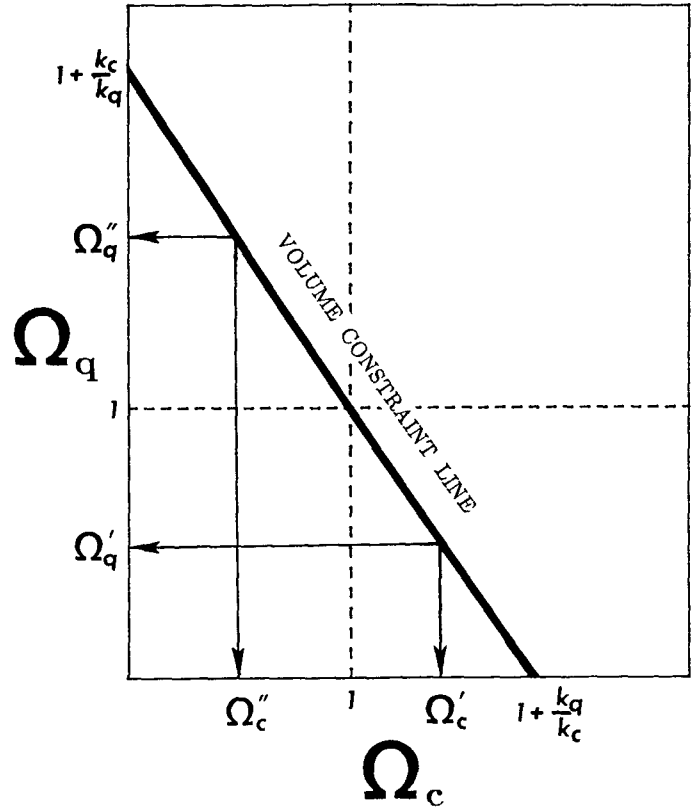

Figure 1. Pressure-of-crystallization "phase diagram" for calcite (c) - quartz (q) rock. Volume constancy implies univariant condition in space of saturation levels (or ratio of activity product to equilibrium constant). Imposed oversaturation of pore fluid with respect to quartz (Ω_q'') would result in undersaturation with respect to calcite (Ω_c''), magnitude of which is determined by Ω_q'' and ratio of rate coefficients k. Similarly, oversaturation with respect to calcite (Ω_c') would produce undersaturation with respect to quartz (Ω_q').

then horizontally to the intersection of the vertical axis at Ω_q'. As the line representing equation 8 passes through the intersection of the quartz and calcite saturation lines, any supersaturation of fluid with respect to calcite imposed on the system would induce an undersaturation with respect to quartz, the magnitude of which depends on the reaction kinetics of both minerals and the level of imposed supersaturation. The converse relation, of course, will also hold: an undersaturation in the pore fluid with respect to calcite, Ω_c'', will result from a supersaturation in the pore fluid with respect to quartz, Ω_q''.

NUMERICAL SIMULATIONS OF CONCRETION GROWTH

To explore more thoroughly the replacement dynamics implied by the pressure of crystallization, we present results on the silicification of limestones via the growth of quartz nuclei in a medium initially saturated with respect to amorphous silica. The latter represents sponge spicules or radiolarians as per Maliva and Siever (1988). The spatial distribution of siliceous concretions is commonly linked to localities originally rich in such high free-energy silica sources (Coniglio, 1987). We limit our considerations to the time following the localized nucleation of quartz. No rock flow is imposed at the boundary of the simulation domain. Solute transport is assumed to be solely diffusional. In addition to the Navier-Stokes equation (equation 2), which arose from conservation of momentum con-

siderations, we require the equations accounting for conservation of mass. Letting L_i represent the radius of a typical i grain and c_α' the aqueous concentration of α in mol/pore volume, conservation of mass yields (see Dewers and Ortoleva, 1989a, for details)

$$\frac{\partial L_i}{\partial t} = G_i \qquad (9)$$

$$\vec{\nabla} \cdot \{\phi D_\alpha \vec{\nabla} c_\alpha\} + \sum_{i=1}^{M} \nu_{\alpha i}\, \rho_i n_i 4\pi L_i^2 G_i = 0, \qquad (10)$$

where G_i is the radial growth rate for mineral i, ϕ is porosity, and D_α is the diffusion coefficient for pore-fluid solute α. For the quartz, calcite, and amorphous silica system ($M = 3$), the reaction network is taken to be

quartz $\rightleftharpoons$ SiO$_2$
amorphous silica $\rightleftharpoons$ SiO$_2$ $\qquad\qquad$ (11)
calcite $\rightleftharpoons$ Ca^{2+} + CO$_3^{2-}$.

We have solved the conservation equations for each mineral and solute species simultaneously by a finite backward difference method. The spatial distribution of pressure P^m was calculated algebraically at the beginning of each time step by applying equation 6 to the three-mineral

system. If we assume equilibrium between the concentrations of Ca^{2+}, CO$_3^{2-}$ (which, for a closed system, is related to $C_{Ca^{2+}}$ via carbonate equilibria) and calcite and between SiO$_2$ and amorphous silica, we regain from equation 6 an expression similar to equation 1 that applies to quartz, for the form of k and Ω in Appendix 1.

A typical simulation is shown in Figure 2 for a spherically symmetric system, r being the radial coordinate. We consider a situation wherein quartz has nucleated in the vicinity of the origin; we follow the postnucleation genesis of a siliceous "concretion" that grows there. A localized region of calcite dissolution accompanying quartz growth is seen to evolve after 16.7 ka. An abrupt transition develops that separates the domain of quartz growth and calcite dissolution from that of calcite growth and dissolution of amorphous silica, marked by a discontinuity in the reaction-mediated pressure. The region of calcite growth may be likened to a calcification front (so denoted by Maliva and Siever, 1987) that arises adjacent to zones of silicification, or in this case, a concretion. The c_{SiO_2} profile, initially at equilibrium with amorphous silica, follows closely the volume fraction profile of the amorphous silica. The $c_{Ca^{2+}}$ profile shows that calcite activity is highest in the region of quartz growth. The resulting concentration gradients drive, via down-gradient diffusional transport, the differentiation between quartz and calcite, influencing as well the distribution of pressure.
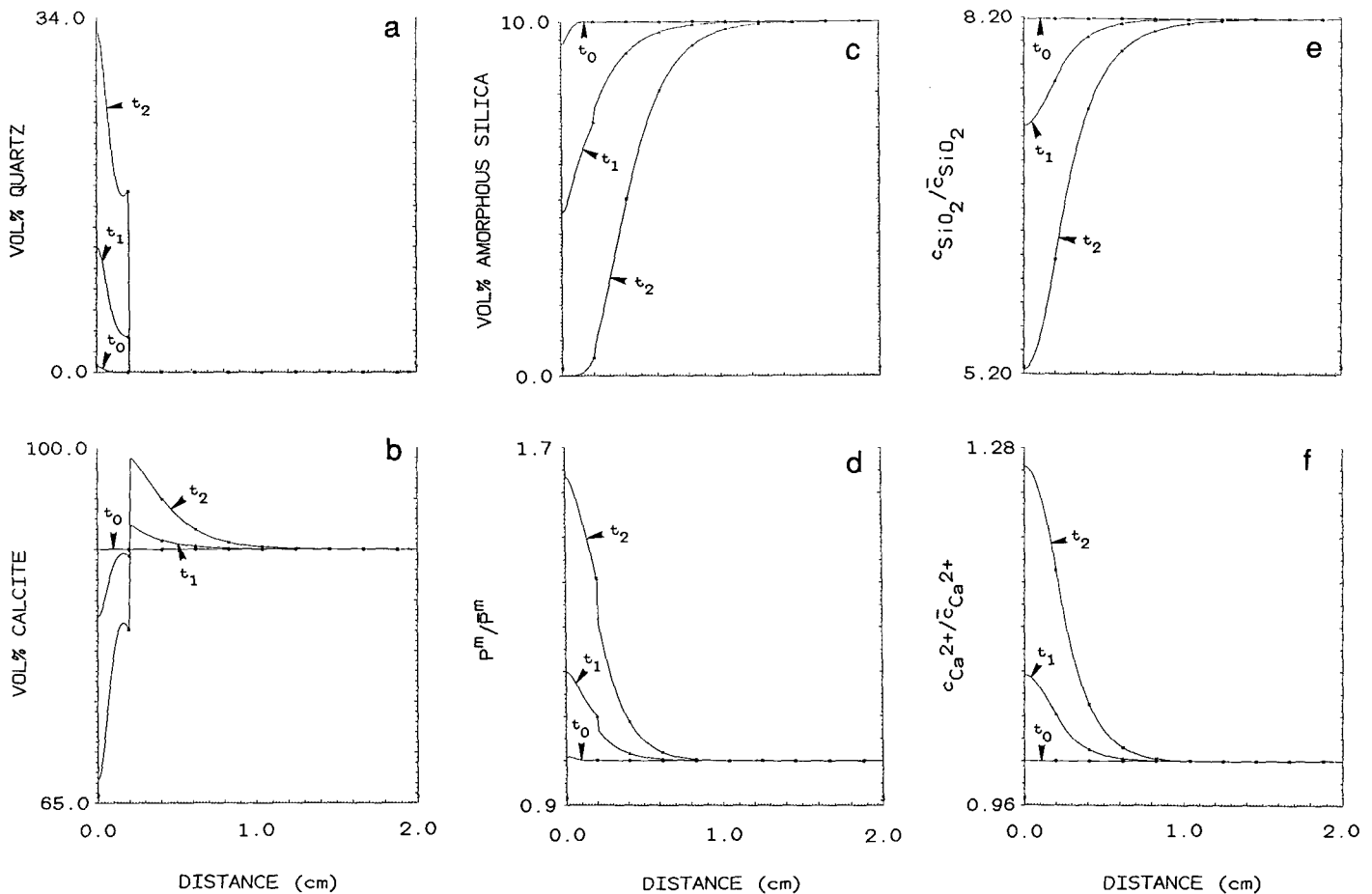

Figure 2. Simulation showing evolution of domain of quartz growth in initially homogeneous rock of calcite plus amorphous silica; t_0 = 0.0 ka, t_1 = 8.3 ka, and t_2 = 16.7 ka. a, b, c: Volume % of quartz, calcite, and amorphous silica. d: Pressure normalized by applied (lithostatic) pressure, $\bar{P}^m$. e: Concentration of SiO$_2$ normalized by concentration of SiO$_2$ in equilibrium with quartz at $\bar{P}^m$. f: Concentration of Ca^{2+} normalized by concentration of Ca^{2+} in equilibrium with calcite at $\bar{P}^m$ under closed-system conditions with pH of 7.

The apparent discontinuity in pressure seen in Figure 2d is a consequence of the large viscosity assumed for the rock. As the viscosity decreases, such a quasi-discontinuity becomes smoothed out. The results show that in stiff rocks, large pressure gradients exist in the vicinity of the concretion/host interface, making this region very active chemically.

The maximum pressure increase at the end of the simulation run is about 33 MPa above the background value of 50 MPa. The limiting stress increase predicted by equation 1 is, from data given in Appendix 1, about 280 MPa, or about a factor of three larger than that obtained from our simulation. This demonstrates the importance of considering the nonequilibrium aspects of the replacement problem, because the stress estimates obtained from the equilibrium result (equation 1; see also Fig. 2 of Maliva and Siever, 1988) represent an upper bound. The stress in our simulation was relieved by calcite dissolution; equilibrium between quartz and pore fluid was not closely approached, and so the stress did not build to a level predicted by the equilibrium condition given in equation 1. By performing other simulations, we have found the maximum stress obtained for a given amount of concretion growth to be inversely proportional to the concentration of Ca^{2+}, which may vary over orders of magnitude depending on, e.g., the partial pressure of carbon dioxide in the pore fluid.

CONCLUSIONS

The simulation of spherical concretion growth presented herein demonstrates that siliceous segregations growing from a high free-energy silica source in a limestone whose mechanical response is sufficiently rigid may proceed over geologic time by local dissolution of that limestone through a pressure-of-crystallization mechanism. The effects of more sophisticated accounts of solution chemistry, lithology, multiphase rock rheology, and crystal growth kinetics on model predictions remain for future investigation.

APPENDIX 1. DATA AND REACTION RATE LAWS USED IN SIMULATION OF FIGURE 2

Equilibrium constants, molar volumes, and other data
$K_{am} = 4.162E-3$ (Fournier and Marshall, 1983)
$K_{qz} = 4.354E-4$ (Fournier and Potter, 1982).

From Plummer and Busenberg (1982):
$K_{ca} = 1.356E-9$; $K_1 = 4.916E-7$; $K_2 = 7.447E-11$.

From Robie et al. (1979): (solid molar densities)
$\rho_{am} = 0.0366$ mol/cm^3; $\rho_{qz} = 0.0441$ mol/cm^3; $\rho_{am} = 0.0271$ mol/cm^3

$T = 343.15$ K   (temperature)
$\bar{P}^m = p = 50$ MPa   (lithostatic and fluid pressures)
$D^c = 2.0E-10$ cm^2/s   (grain boundary diffusion coefficient)
$D = 1.0E-5$ cm^2/s   (pore fluid diffusion coefficient)
$\Delta = 1.0E-7$ cm   (fluid film width; Weyl, 1959)
$\phi = 1.0E-3$ (porosity)
$V_{SiO_2} = 11.00$ mol/cm^3; $V_{CO_3^{2-}} = -7.65$ mol/cm^3 (solute molar volumes).

Relations for reaction rate laws
From Dewers and Ortoleva (1989b) (for use in equation 4):
$k_i = 32\, D_\alpha\, \Delta \tilde{c}_{\alpha i}/L_i^2\, \rho_i$ (rate coefficients, i = calcite, amorphous silica and quartz)
$\Omega_i = c_\alpha/\tilde{c}_{\alpha i}$ (saturations; $\alpha = Ca^{2+}$ for calcite, SiO_2 for amorphous silica and quartz)

$$\tilde{c}_{\alpha i} = \left[\frac{K_i}{\prod_{\beta \neq \alpha} c_\beta^{\nu_{\beta i}}}\right] \exp\left[\frac{(P_{max}-p)}{RT}\left\{\frac{1}{\rho} - \sum_{\beta \neq \alpha} V_\beta \nu_{\beta i}\right\}\right]\; ; \beta \text{ represents } CO_3^{2-}$$

for calcite and $\nu_{\beta i} = 0$ for quartz and amorphous silica.
$P_{max} - p \cong 3\,(P^m - p)$ (P^m is average normal stress across contact, P_{max} is stress at contact center, and p is fluid pressure).
For closed system with constant pH (total calcium equals total carbonate):

$$c_{CO_3^{2-}} = c_{Ca^{2+}}\left\{1 + \frac{10^{-pH}}{K_2} + \frac{(10^{-pH})^2}{K_1 K_2}\right\}^{-1}.$$

REFERENCES CITED

Buczynski, C., and Chafetz, H.S., 1987, Siliciclastic grain breakage and displacement due to carbonate crystal growth: An example from the Lueders Formation (Permian) of north-central Texas, U.S.A.: Sedimentology, v. 34, p. 837–843.
Coniglio, M., 1987, Biogenic chert in the Cow Head Group (Cambro-Ordovician) western Newfoundland: Sedimentology, v. 34, p. 813–823.
Dewers, T., and Ortoleva, P., 1989a, Mechano-chemical coupling via texture dependent solubility in stressed rocks: Geochimica et Cosmochimica Acta, v. 53, p. 1243–1258.
——1989b, Geochemical self-organization III: A mechano-chemical model of metamorphic differentiation: American Journal of Science.
Fournier, R.O., and Marshall, W.L., 1983, Calculation of amorphous silica solubilities at 25° to 300° C and apparent cation hydration numbers in aqueous salt solutions using the concept of effective density of water: Geochimica et Cosmochimica Acta, v. 47, p. 587–596.
Fournier, R.O., and Potter, R.W., III, 1982, An equation correlating the solubility of quartz in water from 25° to 900° C at pressures up to 10,000 bars: Geochimica et Cosmochimica Acta, v. 46, p. 1969–1973.
Maliva, R.G., and Siever, R., 1987, Force of crystallization as a silicification mechanism: Geological Society of America Abstracts with Programs, v. 19, p. 757.
——1988, Mechanisms and controls of silicification of fossils in limestones: Journal of Geology, v. 96, p. 387–398.
Ostapenko, G.T., and Yaroshenko, N.S., 1975, Excess pressure on solid phases generated by hydration (experimental data on hydration of plaster of paris and lime): Geochimica Internationale, v. 12, p. 72–81.
Pettijohn, F.J., 1975, Sedimentary rocks: New York, Harper and Row, 628 p.
Plummer, L.N., and Busenberg, E., 1982, The solubilities of calcite, aragonite, and vaterite in CO_2-H_2O solutions between 0 and 90°C, and an evaluation of the aqueous model for the system $CaCO_3$-CO_2-H_2O: Geochimica et Cosmochimica Acta, v. 46, p. 1011–1040.
Reuss, A., 1929, Berechnung der fliessgrenze von meschkristallen auf grund der plastizitatsbedigung für einkristalle: Zeitschrift für Angewandte Mathematik und Mechanik, v. 9, p. 49–58.
Robie, R.A., Hemingway, B.S., and Fisher, J.R., 1979, Thermodynamic properties of minerals and related substances at 298.15 K and 1 bar (10^5 pascals) pressure and at higher temperatures: U.S. Geological Survey Bulletin, v. 1452, p. 456.
Weyl, P.K., 1959, Pressure solution and the force of crystallization—A phenomenological theory: Journal of Geophysical Research, v. 64, p. 2001–2025.